Original Paper

Inverse determination of glass viscosity and heat transfer coefficient by industrial testing

Dominique Lochegnies and Christophe Marechal
L.A.M.I.H. UMR 8530 CNRS, University of Valenciennes, Valenciennes (France)

In the numerical optimization of a new robotized glass blowing method, convection coefficient and glass viscosity are considered as parameters most influential in the forming process. Consequently, two tests in the industrial framework have been developed. In the first, the temperature is measured by a pyrometer on a glass ingot moved in rotation by the robot. In the second one, the robot holds the glass ingot vertically and the lengthening of the glass is recorded by video camera. In both cases, numerical modelling coupled with the inverse method completes the identification procedure. Finally, the integration of the identified properties in the modelling of the elongation of the glass considerably improves the representation of the real glass flow.

1. Introduction

To answer an increasing need for glass product manufacturing in both small and medium series, the first glass-blowing robot has recently been developed by the French company Cyberglass Robotics. This first specimen, used in production since July 2000 in crystal glass manufacturing in Slovenia, gives a very high degree of flexibility and authorizes the manufacturer to produce a wide range of articles, pushing away the current limitations on weight and shape. The robotized forming process consists of three stages:

- reheating of the glass ingot at the furnace exit,
- parison forming,
- final blowing in a product-shaped mould.

In the face of this new technology, which particularly interests crystal glass-makers, experiments remain the main decision-making element for the design of the robotized forming process. To reduce the adjustment time, a numerical approach based on the finite element models of the new technique glass blowing has been developed [1 and 2].

First of all, a sensitivity analysis is performed in order to find the parameters most influential in the blowing success, which is expressed as a glass distribution in the final product in agreement with the designer's specifications. According to the numerical sensitivity analysis, the coefficient of convection between the hot glass and the ambient air and the glass viscosity law are among the most influential material properties.

Received 1 October 2001, revised manuscript 30 July 2002.

For a long time, industrial and academic research has been done in different fields of glass forming. In 1925, Vogel, Fulcher and Tammann were the first to quantify the thermal dependence of the glass viscosity $\eta(\vartheta)$ in a temperature range from 500 to 1400 °C [3]. They used a logarithmic law, well-known as VFT (Vogel/Fulcher/Tammann) equation:

$$\lg(\eta) = -A + \frac{B}{(T - T_o)} \tag{1}$$

where A, B and T_o are constants depending on the nature of glass. Thereafter, this model has been used to identify the viscosity of various kinds of glasses for other temperature ranges according to experimental processes:

- by falling-ball viscosimetry between 700 and 900 °C [4],
- by fibre elongation [5] or cone-plate rheometry between 530 and 800 °C [6],
- by cylinder compression between 580 and 660 °C [7].

In addition to the temperature, viscosity strongly depends on the glass composition. Lakatos et al. studied this dependence and determined a relation between the A, B, T_o constants and the percentage of elements which composed a sodacalcic [8] and a crystal glass [9 to 11].

Heat exchange in glass is the second point on which many studies have been undertaken. As with the viscosity, the thermal parameters are dependent on the glass composition and the temperature. In 1951, Sharp and Ginther showed this dependence for the specific heat [12] in the temperature range of 0 to 1300 °C. On the one hand, real conductivity can be given only for a

temperature range from 0 to 600 °C [13]. Beyond that, the radiation can not be considered as negligible. So the real conductivity is replaced by the effective conductivity determined from the diffusivity measurement [14].

During the forming process, glass cooling varies depending on time in the ambient air and contact with the moulds. For these exchanges by convection and conduction, two effects are combined:

a) cooling following the contact of the two bodies and very significant at high temperatures,
b) heating caused by the thermal radiation of the glass.

In the case of the glass exposed to ambient air, an equivalent convection coefficient can be used to couple these two effects [15]. It evolves linearly and is obtained by adding the heat quantity lost by convection and radiation. The total heat quantity is then dependent on the air temperature, the glass surface temperature and the equivalent convection coefficient. In the case of contact between the glass and a mould, the thermal heat is dependent on the temperature of the two bodies, but also on the contact surface quality and the nature of the materials. In 1961 McGraw established a law for this heat transfer as a function of the contact time [16].

Based on an inverse method applied to the identification of the properties of materials (viscoplastic property of an alloy aluminium [17], rheological property of a steel [18], hardness estimation by a tension test [19], elastic property of a cylindrical inclusion [20]), the identification tools were first of all extended to the determination of the rheological properties of glass used in the numerical modelling of tempering [21]. Thereafter, this method was used to identify the optimum adjustment parameters of glass forming processes. Such optimizers can now be used for a wide range of industrial objectives to:

- obtain a state of internal stress after the tempering of a flat glass [21],
- determine the optimum geometry of a parison to obtain a thickness distribution at the end of the robotized forming process [22].

In this paper, we present two tests developed in the industrial framework for the identification of the properties of convection and glass viscosity. The identification procedure is achieved by numerical modelling of the tests coupled with the inverse method.

2. Industrial testing of the convection

To determine the coefficient of convection with the ambient air, the temperature evolution on the ingot surface is taken. The robot brings the glass ingot to a horizontal position with a continuous rotation of its arm which prevents the flowing of the glass (figures 1a and b).

The experimental procedure is broken down into a phase of transfer between the furnace and the position

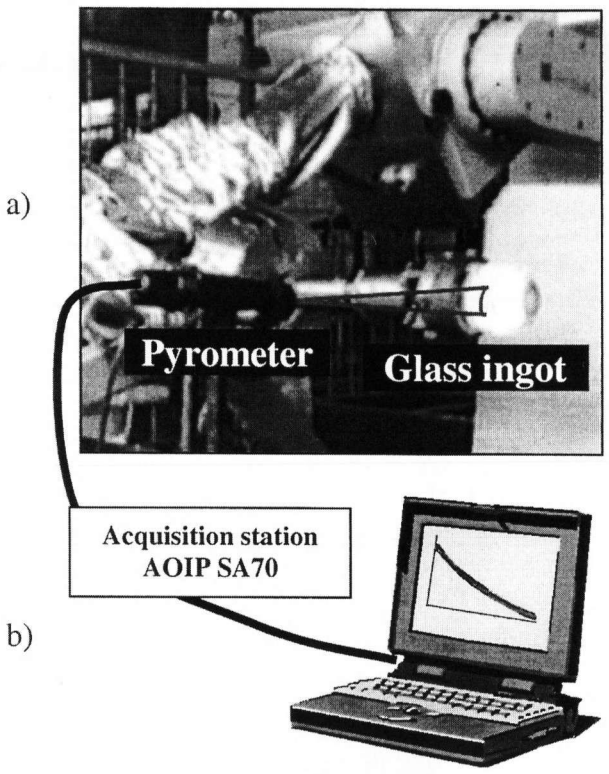

Figures 1a and b. Principle and method of measurement for the industrial testing of the convection coefficient; a) measurement principle, b) acquisition system.

of measurement, followed by a phase of cooling without ingot deformation. A pyrometer TXG5 (AS Technologie Langlade (France)) is used to take the temperature measurement. This pyrometer has a wavelength of 5 μm which allows one to take the temperature measurement on the glass surface. The pyrometer is connected to an acquisition station (A.O.I.P. SA 70). With a frequency of acquisition of 0.14 s, seven readings are taken each second. Each data collection lasts 6 min 30 s, in order to cover the temperature field (500 to 850 °C).

With an arm rotation speed of 40 rpm, the same point of the ingot periphery has an appearance cycle in front of the pyrometer of 1.5 s with a measurement cycle of 3 s. We can observe a slight temperature fluctuation due to the transfer of the ingot between the furnace and the measurement point. The curves of figures 2a and b give the cooling on the surface of the ingot during the tests. From these curves, we extract an average temperature evolution which represents the objective of the identification.

To get several initial temperatures of the ingot at the furnace exit, tests are carried out for various heating times from 4 to 10 s. For each heating time, only one acquisition is made per ingot, except for 8 and 10 s of heating, where two tests are carried out. In order to identify the convection coefficient, cooling is simulated by a nonstationary 1D axisymmetric thermal model using the finite difference method in explicit formulation

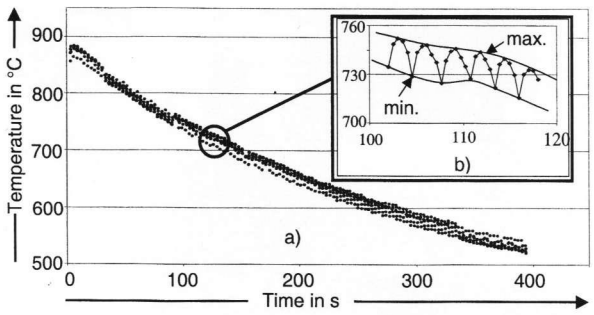

Figures 2a and b. Acquisition of the surface temperature of an ingot; a) complete acquisition, b) appearance cycle in front of the pyrometer (section 100 to 120 s as marked in a)).

[23]. The material properties for this modelling are listed in section 7.1. The glass ingot's diameter is 0.07 m. The finite difference model is composed of 11 nodes distributed regularly with a gap of $\Delta R = 0.0035$ m between each of term (figures 3a and b).

The total cooling time varies from 396 to 400 s. The numerical simulation begins with a transfer phase from the furnace to the reading position and a period from 5 to 9 s where the acquisition station begins reading. During this first phase, the ingot is in heat exchange with the ambient air for a period of time varying from 15 to 19 s.

The aim of the identification is to determine three parameters:

- ϑ_{init}: initial temperature of the glass ingot,
- a and b: parameters describing the convection coefficient $h(\vartheta)$ by a linear law: $a\vartheta+b$ [15].

The identification of these parameters $N=3$ is undertaken to reduce the difference between the result of the finite difference model and the temperature readings.

The number of comparison points M is 128, which largely respects the conditions for use of the identification method, i.e. a number of comparison points M superior or equal to the number of parameters N.

The identification is carried out by minimization of the error function $E(\vartheta_{init}, a, b)$ defined by:

$$E(\vartheta_{init}, a, b) \equiv \frac{1}{2} \sum_{s=1}^{M} (\vartheta_s^*(\vartheta_{init}, a, b) - \hat{\vartheta}_s)^2 \qquad (2)$$

with $\vartheta_s^*(\vartheta_{init}, a, b)$ the response of the numerical simulation for the surface node at the moment t_s, and $\hat{\vartheta}_s$ the experimental reading of the surface temperature at the same moment.

Selected initial values to start the identification method are:

- initial temperature $\vartheta_{init} = 1000\,°C$,
- $a = 0.22\ W\,m^{-2}\,K^{-2}$ and $b = -64\ W\,m^{-2}\,K^{-1}$, values deduced from the evolution of the convection coefficient $h(t)$ proposed by César De Sa [15].

At the beginning of the identification, the coefficient of sensitivity S_p and the Levenberg-Marquardt parameter λ are 0.01 and 0.1, respectively.

The identification of ϑ_{init}, a and b, for each acquisition, requires between four and five iterations. Table 1 recapitulates the results obtained for each test. The average gap ΔE which represents the average error between the solution of the simulation with the identified parameters, and the experimental reading, is calculated by:

$$\Delta E(\vartheta_{init}, a, b) = \sqrt{\left(\frac{2 \cdot E(\vartheta_{init}, a, b)}{M}\right)}. \qquad (3)$$

The average gap gives a better representativeness of the identification quality than the error function. For the

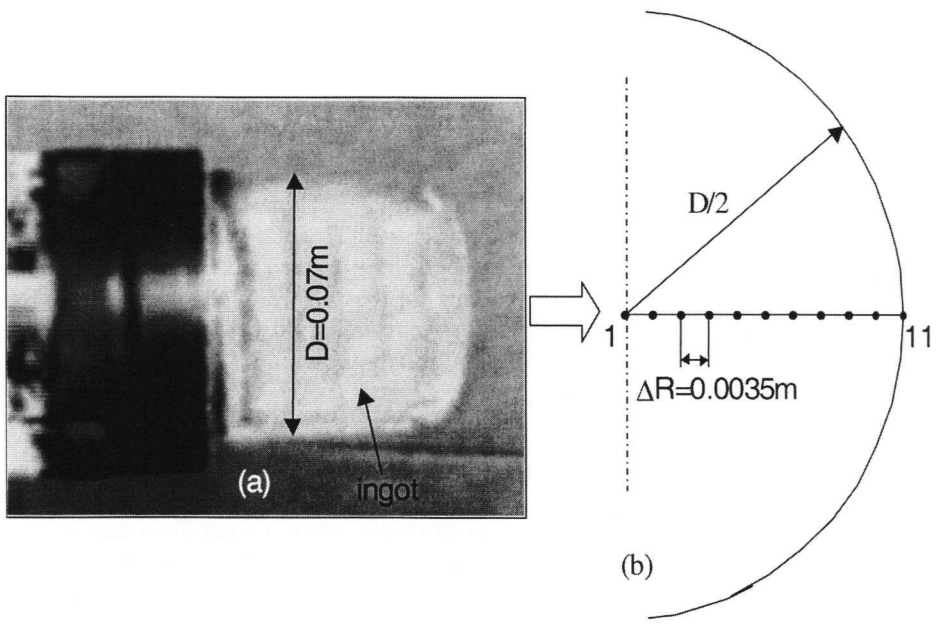

Figures 3a and b. Glass ingot for the industrial testing of the convection; a) real view, b) axisymmetric thermal finite difference model.

Table 1. Identification results of a, b, ϑ_{init}

heating time in s	4	5	6	$8_{test\ 1}$	$8_{test\ 2}$	$10_{test\ 1}$	$10_{test\ 2}$
a in W m^{-2} K^{-2}	0.128	0.135	0.142	0.151	0.141	0.112	0.112
b in W m^{-2} K^{-1}	−18.04	−23.40	−27.18	−30.70	−26.44	−13.06	−15.89
ϑ_{init} in °C	940	950	945	945	954	942	949
error	196	167	220	248	210	231	268
iterations	5	4	4	4	4	4	4
average gap ΔE in K	1.76	1.62	1.86	1.98	1.82	1.91	2.05

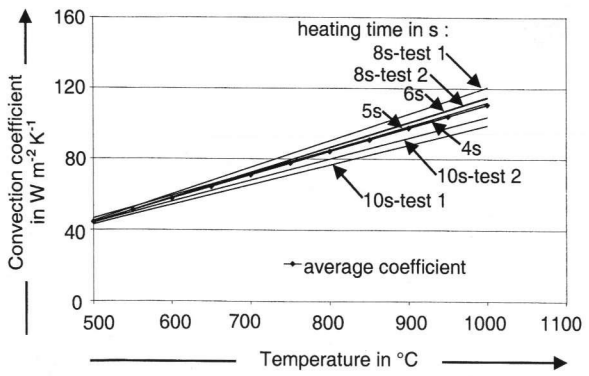

Figure 4. Evolutions of identified convection coefficients according to the model $h = a \cdot \vartheta + b$ for the tests and average convection coefficient $h_a = a_a \cdot \vartheta + b_a$.

various tests, the identification of each convection coefficient gives an average gap lower or equal to 2 K (table 1), which corresponds to an average error of 0.4% for an average temperature at the end of the reading of 518 °C. The different evolutions from each coefficient identified are due to the modifications of the measurement conditions and also to an ingot temperature which is not perfectly homogeneous.

To be able to use the convection coefficient for the numerical modelling of the robotized blowing [2], an average convection coefficient is deduced from the previous identification (table 1) and the evolution of this average convection coefficient $h_a(\vartheta)$ (figure 4) is described by the linear law given as:

$$h_a(\vartheta) = a_a \cdot \vartheta + b_a = 0.1328 \cdot \vartheta - 22.06 \qquad (4)$$

with a_a and b_a as average parameters describing the linear dependency of $h_a(\vartheta)$ in regard to the temperature ϑ (figure 4).

With this average convection coefficient, an identification of the initial temperature is carried out for all tests. Then, according to the average convection coefficient identified, determination of the initial glass temperature is carried out a second time for each heating time. Indeed, for this identification, the heating temperatures are the same (4, 5 and 6 s).

The identification of the initial temperatures gives the determination of the relation between the heating time and the initial temperature. Thus it is possible to identify the initial temperature according to the heating time included in the interval of identification of 4 to 10 s. The values of initial temperature used for the viscosity identification are:

- $\vartheta_{init}(4\ s) = 936\,°C$,
- $\vartheta_{init}(5\ s) = 940\,°C$,
- $\vartheta_{init}(6\ s) = 943\,°C$.

3. Industrial testing of the glass viscosity

For the viscosity identification, the glass ingot is put in a vertical position after heating, to be able to lengthen it under its own weight. In this case, the experimental procedure consists of a phase of transfer between the furnace and the creep position, followed by a lengthening phase of the ingot without rotation of the robot arm. To measure the lengthening, a video camera is placed in front of the ingot during the vertical creep (figure 5). The video recordings are digitalized in order to be able to extract:

- the shape of the ingot before creep,
- the lengthening of the lowest point of the ingot.

The first information is used to define the initial geometry of the ingot for the finite element model. The second information provides the objective of the identification.

For each heating time, the lengthening of the glass ingot is read at the lowest point according to time. Three phases of lengthening evolution (phase 1: acceleration, phase 2: stabilization and phase 3: deceleration) are found for the three different heating times (figure 6). The temperature increase only influences the lengthening levels obtained.

Thus the same modelling is used for the three types of tests and only the initial temperature of the ingot is modified. The lengthening test is simulated by an axisymmetric thermomechanical finite element model using Abaqus software. The finite element mesh is composed of 900 elements with four axisymmetric nodes and four integration points (figure 7).

There are two stages to the simulation:

- the first one simulates the transfer between the furnace and the position of measurement with only heat transfer phenomena,

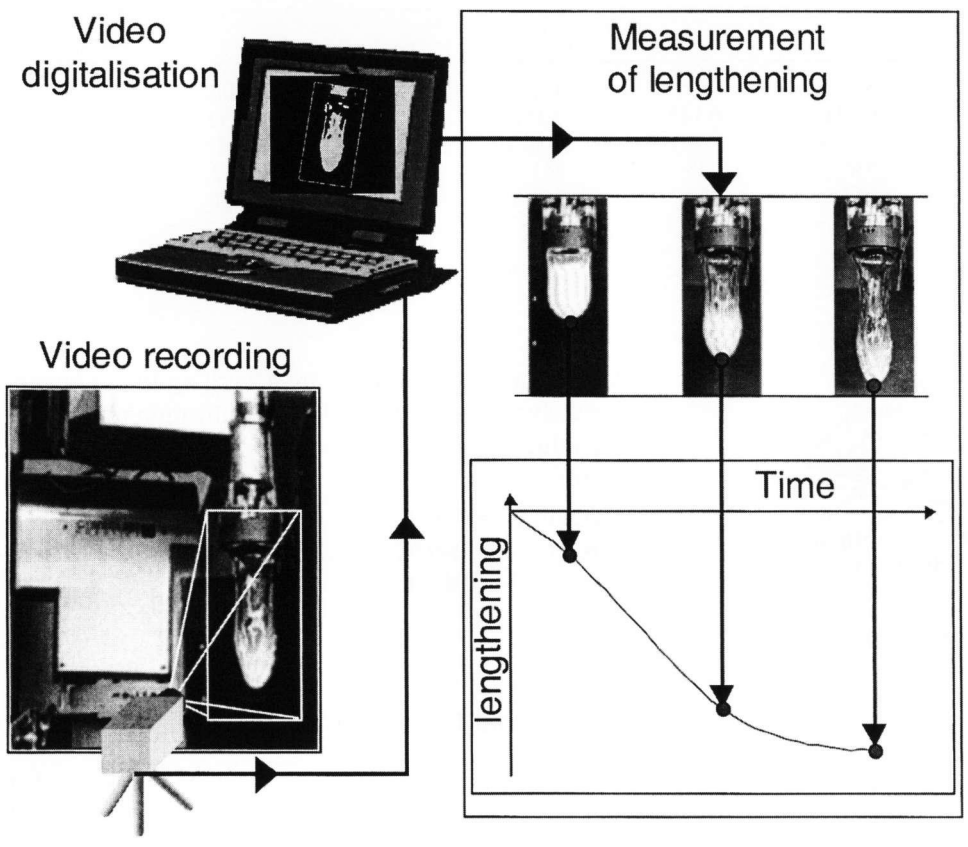

Figure 5. Principle and method of measurement on a glass ingot for the rheological tests of the glass viscosity.

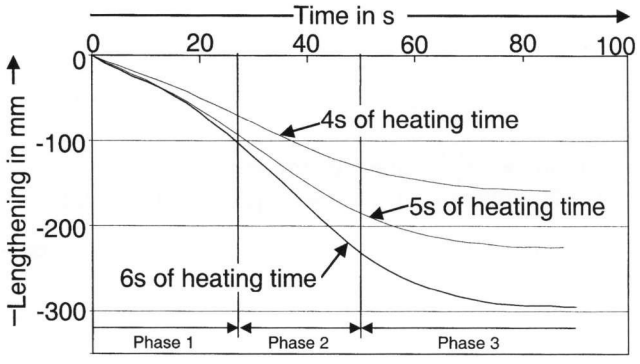

Figure 6. Lengthening of the glass ingot measured for various heating times.

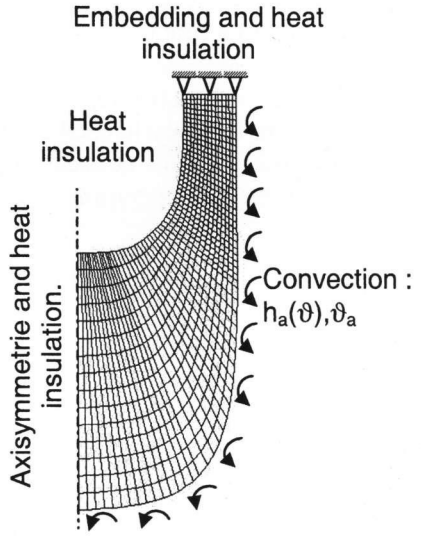

Figure 7. Meshing of the glass ingot and boundary conditions of the finite element model for the viscosity identification.

— the second one reproduces the lengthening of the glass ingot in complete thermomechanical coupling.

The various material properties for the finite element model are listed in section 7.1. The initial temperature and the average convection coefficient given in equation (4) are used.

The viscosity identification is carried out on viscosity/temperature couples (η_i, ϑ_i). To avoid large differences between viscosities ($2.91 \cdot 10^3$ Pa s with 1000 °C, $7.26 \cdot 10^{+9}$ Pa s with 600 °C), the identification is made for three fields of temperatures in each phase observed on the lengthening curves (figure 6) to get a good representativeness of the glass viscosity law. The error functions minimized for the three lengthening phases are given by:

phase 1:

$$E_1(\eta_1, \eta_2, \eta_3, \eta_4) = \frac{1}{2} \sum_{s=1}^{M_1} \left(u_s^*(\eta_1, \eta_2, \eta_3, \eta_4) - \hat{u}_s \right)^2, \quad (5)$$

phase 2:

$$E_2(\eta_4, \eta_5, \eta_6) = \frac{1}{2} \sum_{s=1}^{M_2} \left(u_s^*(\eta_4, \eta_5, \eta_6) - \hat{u}_s \right)^2, \quad (6)$$

phase 3:

$$E_3(\eta_6, \eta_7, \eta_8, \eta_9) = \frac{1}{2} \sum_{s=1}^{M_3} \left(u_s^*(\eta_6, \eta_7, \eta_8, \eta_9) - \hat{u}_s \right)^2 \quad (7)$$

where u_s^* is the solution to the finite element simulation in terms of lengthening of the lowest point of the ingot, and $\hat{u}_s$ the lengthening measured at the same moment t_s. The inverse method (section 7.2) is now adapted to minimize the error functions E_1 (5), E_2 (6) and E_3 (7).

The temperature values used for each phase of the identification are:

- phase 1: $\vartheta_1 = 950\,°C$, $\vartheta_2 = 925\,°C$, $\vartheta_3 = 900\,°C$ and $\vartheta_4 = 870\,°C$, for a length of 27.5 s and $M_1 = 10$ comparison points,
- phase 2: $\vartheta_4 = 870\,°C$, $\vartheta_5 = 820\,°C$ and $\vartheta_6 = 770\,°C$, for a length of 50 s and $M_2 = 24$ comparison points,
- phase 3: $\vartheta_6 = 770\,°C$, $\vartheta_7 = 720\,°C$, $\vartheta_8 = 700\,°C$ and $\vartheta_9 = 670\,°C$, for a length of 85 s and $M_3 = 33$ comparison points.

The last temperature of a field is the first of the following phase to ensure the continuity between the phases. For phase 3, the viscosity at 500 °C, calculated by the VFT law (table 5, see section 7), is added to limit the effect of the boundary values.

For the different identifications, the Levenberg-Marquardt parameter is worth 10 and the sensitivity coefficient is equal to 0.05 for phase 1, 0.5 for phase 2, and 0.1 for phase 3. For each phase, with large differences between viscosities, different values for each sensitivity coefficient must be used.

For each heating time, three identifications of the couples (η_i, ϑ_i) are used. For the first identification phase, the initial values of the four couples (η_i, ϑ_i) are:

- for the first identification (heating time of 4 s) calculated from the VFT law (table 5, see section 7),
- for the second identification (heating time of 5 s) given by the first identification,
- for the third identification (heating time of 6 s) given by the second identification.

For phase 2 the A, B and T_o parameters of the VFT law (equation (1)) are determined thanks to the couples (η_i, ϑ_i) identified by the first phase. The initial values of the three couples (η_i, ϑ_i) of phase 2 are calculated by extrapolating the determined VFT law at the temperature ϑ_i. For phase 3, the same determination is carried out by the calculation of the initial values of the four couples (η_i, ϑ_i) to be identified. The identification converges to a good solution after a number of iterations. All results obtained are recapitulated for the three phases in tables 2, 3 and 4, respectively. For heating times of 4, 5 and 6 s, the average gap ΔE (equation (3)) is respectively 1.32, 1.65 and 3.22 mm. The final lengthening for 4 s of heating time is 158 mm, for 5 s of heating time 225 mm and for 6 s of heating time 294 mm. The relation between this final lengthening and the average gap is 0.8, 0.7 and 1.1 % for 4, 5 and 6 s of heating time, respectively. These variations are very small and figure 8 clearly shows that the lengthenings, calculated by the finite element simulation with the identified viscosities, are very close to the experimental lengthenings.

Figure 9 shows the identified viscosities and the average viscosity computed from tables 2, 3 and 4 for each temperature level. The differences between the identified values for the different tests at a temperature above 750 °C are low (inferior to $24.05 \cdot 10^3$ Pa s). Below this temperature, the variation increases specially for the viscosity identified in phase 3, where lengthening is stabilized. As the working temperature range of glass is

Table 2. Identification results for phase 1, field 1

		heating time in s		
		4	5	6
viscosity in Pa s	η_1	$4.84 \cdot 10^3$	$5.71 \cdot 10^3$	$7.65 \cdot 10^3$
	η_2	$1.41 \cdot 10^4$	$1.35 \cdot 10^4$	$1.45 \cdot 10^4$
	η_3	$2.50 \cdot 10^4$	$2.34 \cdot 10^4$	$2.38 \cdot 10^4$
	η_4	$5.87 \cdot 10^4$	$5.31 \cdot 10^4$	$5.04 \cdot 10^4$
error		$1.12 \cdot 10^{-5}$	$1.27 \cdot 10^{-5}$	$2.19 \cdot 10^{-5}$
iterations		25	19	20
average gap ΔE in mm		1.49	1.59	2.09

Table 3. Identification results for phase 2, field 2

		heating time in s		
		4	5	6
viscosity in Pa s	η_4	$5.34 \cdot 10^4$	$4.83 \cdot 10^4$	$4.69 \cdot 10^4$
	η_5	$7.03 \cdot 10^4$	$6.74 \cdot 10^4$	$6.15 \cdot 10^4$
	η_6	$2.37 \cdot 10^5$	$2.49 \cdot 10^5$	$2.25 \cdot 10^5$
error		$2.87 \cdot 10^{-5}$	$4.02 \cdot 10^{-5}$	$4.76 \cdot 10^{-5}$
iterations		34	32	56
average gap ΔE in mm		1.55	1.83	1.99

Table 4. Identification results for phase 3, field 3

		heating time in s		
		4	5	6
viscosity in Pa s	η_6	$2.15 \cdot 10^5$	$2.19 \cdot 10^5$	$1.89 \cdot 10^5$
	η_7	$7.14 \cdot 10^5$	$4.22 \cdot 10^5$	$3.74 \cdot 10^5$
	η_8	$2.23 \cdot 10^6$	$6.63 \cdot 10^6$	$3.94 \cdot 10^6$
	η_9	$3.51 \cdot 10^7$	$6.59 \cdot 10^7$	$4.06 \cdot 10^6$
error		$2.88 \cdot 10^{-5}$	$4.53 \cdot 10^{-5}$	$1.72 \cdot 10^{-4}$
iterations		24	26	21
average gap ΔE in mm		1.32	1.65	3.22

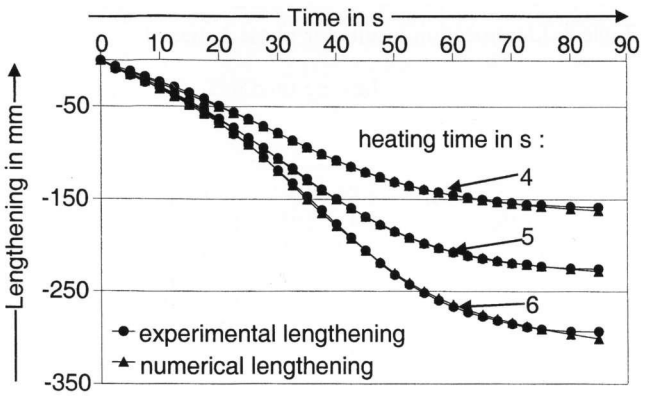

Figure 8. Lengthenings calculated by the finite element simulation with the identified viscosities, and experimental lengthenings.

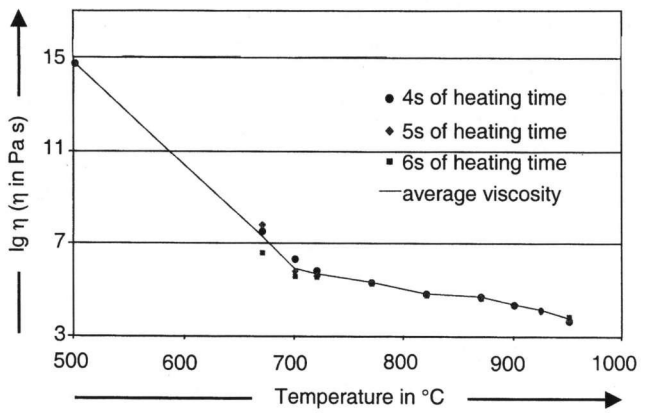

Figure 9. Identified viscosities for various heating times and average viscosity.

higher than 800 °C, average viscosity can be used in the modelling of the robotized glass blowing.

To check that this average does not generate large errors, lengthening for the three tests is recomputed with the finite element model. The same calculation is implemented with the viscosity given by the VFT law (table 5, see section 7) to determine whether the identification

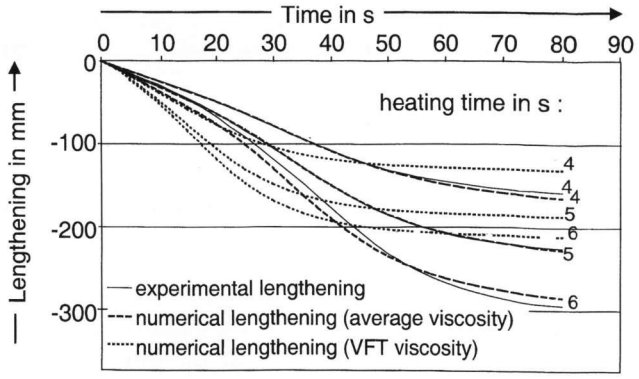

Figure 10. Experimental lengthening and lengthening calculated by the finite element model with the average viscosities and the viscosities given by the VFT law.

improves the simulation or not. Figure 10 shows that the lengthening obtained with the average viscosity better reproduces the experimental lengthening. The average gap ΔE (equation 3)) is divided by 5.6 for 4 s of heating time, 13 for 5 s of heating time, and 3.2 for 6 s of heating time, respectively.

Identification significantly reduces the error between the numerical and experimental results. The finite element models are considerably improved to optimize a forming process for example.

4. Conclusions

For the identification of two glass properties, convection with air and viscosity law as functions of temperature, two original tests have been developed in the industrial framework employing a blowing robot.

For the first test, using the inverse method and finite difference modelling, the average convection is identified by means of pyrometer measurements. For the second one, in which the inverse method is applied to thermo-mechanical finite element modelling and which is based

Table 5. Glass material properties and respective values

material properties	symbols	values
density in kg/m^3	ϱ_v	2494
specific heat in J kg^{-1} K^{-1}	$C_v(\vartheta)$	$\dfrac{2.9353 \cdot 10^{-3}\,\vartheta^2 + 4.0209 \cdot \vartheta + 699.05}{(0.00146 \cdot \vartheta + 1)^2}$
conductivity in W m^{-1} K^{-1}	$k_v(\vartheta)$	1.01 1.45 1.94
	$\vartheta < 600\,°C$	0 300 600
	$k_v^*(\vartheta)$	4.53 9.35 20.7 42.03 65.04
	$\vartheta > 600\,°C$	700 900 1100 1300 1400
viscosity in Pa s	$\eta(\vartheta)$	$\lg(\eta) \equiv -1.9458 + \dfrac{5407}{(\vartheta - 174.5)}$
convection/air coefficient in W m^{-2} K^{-1}	$h_a(\vartheta)$	$0.22 \cdot \vartheta - 64$

on video camera recording, the average glass viscosity law is clearly identified. Finally, the integration of the identified properties in the modelling of the elongation of the glass ingot has considerably increased the representation of the real glass flow.

*

The present work is supported by the CNRS, the European Community, the Ministère de L'Education Nationale et de la Recherche, the Laboratoire d'Automatique, de Mécanique et d'Informatique Industrielles et Humaines and the Cyberglass Robotics Company. The authors gratefully acknowledge the support of these institutions.

5. References

[1] Marechal, C.; Lochegnies, D.; Oudin, J.: Finite element models for robotics in hollow glass forming. In: Proc. International Colloquium on Modelling of Glass Forming Processes, Valenciennes 1998, p. 181–190.
[2] Marechal, C.; Lochegnies, D.; Oudin, J.: Numerical optimization of a new robotized glass blowing. In: Proc. 5th Conference of the European Society of Glass Science and Technology, (ESG) Prague 1999, p. 44–50.
[3] Fulcher, G. S.: Analysis of recent measurements of the viscosity of glasses. J. Am. Ceram. Soc. **8** (1925) no. 6, p. 339–355.
[4] Bré, M.: Caractérisation de la viscoélasticité des verres. Verres Réfract. **31** (1977) no. 6, p. 671–680.
[5] Simmons, J. H.; Mohr, R. K.; Montrose, C. J.: Non-Newtonian viscous flow in glass. J. Appl. Phys. **53** (1982) no. 6, p. 4075–4080.
[6] Simmons, J. H.; Ochoa, R.; Simmons, K. D. et al.: Non-Newtonian viscous flow in soda-lime-silica glass at forming and annealing temperature. J. Non-Cryst. Solids **105** (1988) no. 3, p. 313–322.
[7] Manns, R.; Brückner, R.: Non-Newtonian flow behaviour of a soda-lime silicate glass at high deformation rates. Glastech. Ber. **61** (1988) no. 2, p. 46–56.
[8] Scholze, H.: Glass : nature, structure, and properties. New York et al.: Springer, 1991.
[9] Lakatos, T.; Johansson, L. G.; Simmingsköld, B.: Investigation on viscosity-temperature relations in the lead crystal system containing 24–30% PbO. Pt I. Glastek. Tidskr. **32** (1977) no. 2, p. 31–35.
[10] Lakatos, T.; Johansson, L. G.; Simmingsköld, B.: Investigation on viscosity-temperature relations in the lead crystal system containing 24–30% PbO. Pt II. Glastek. Tidskr. **33** (1978) no. 3, p. 55–59.
[11] Lakatos, T.; Johansson, L. G.; Simmingsköld, B.: Investigation on viscosity-temperature relations in the lead crystal system containing 24–30% PbO. Pt III. Glastek. Tidskr. **34** (1979) no. 1, p. 9–11.
[12] Sharp, D. E.; Ginther, L. B.: Effect of composition and temperature on the specific heat of glass. J. Am. Ceram. Soc. **34** (1951) no. 9, p. 260–271.
[13] Primenko, V. I.: Theoretical method of determining the temperature dependence of the thermal conductivity of glasses. Steklo Keram. (1980) no. 5, p. 17–18.
[14] Van Zee, A. F.; Babcock, C. L.: A method for the measurement of thermal diffusivity of molten glass. J. Am. Ceram. Soc. **34** (1951) p. 244–250.
[15] Cesar De Sa, J. M. A.: Numerical modelling of glass forming processes. Eng. Comput. **3** (1951) no. 6, p. 266–275.
[16] McGraw, D. A.: Transfer of heat in glass during forming. J. Am. Ceram. Soc. **44** (1961) no. 7, p. 353–363.
[17] Gelin, J. C.; Ghouati, O.: An inverse method for determining viscoplastic properties of aluminium alloys. J. Mater. Provess. Technol. **45** (1994) no. 1–4, p. 435–440.
[18] Gavrus, A.; Massoni, E.; Chenot, J. L.: Computer aided rheology for constitutive parameter identification. In: Proc. IVth Computational Plasticity Fundamentals and Applications, Barcelona 1995, p. 755–766.
[19] Rodic, T.; Gresovnik, I.; Owen, D. R. J.: Application of error minimization concept to estimation of hardening parameters in the tension test. In: Proc. IVth Computational Plasticity Fundamentals and Applications, Barcelona 1995, p. 779–786.
[20] Schnur, D. S.; Zabaras, N.: An inverse method for determining elastic material properties and a material interface. Int. J. Numer. Methods Eng. **33** (1992) no. 10, p. 2039–2057.
[21] Lochegnies, D.; Wiertel, P.; Narayanaswamy, O. S.: Inverse determination of material properties and optimization of flat glass tempering. Int. J. Form. Processes **2** (1999) no. 1–2, p. 95–116.
[22] Moreau, P.; Marechal, C.; Lochegnies, D.: Optimum parison shape for glass blowing. Proc. XIX International Congress on Glass, Edinburgh 2001. Ext. Abstracts, p. 548–549.
[23] De Vriendt, A. B.: La transmission de chaleur. Quebec: Gaëtan Morin, 1984, p. 576–585.

6. Appendices

6.1 Set of material properties for the numerical modelling of the industrial tests

The set of glass material properties used for the process modelling are listed in table 5. This set of properties are proposed by:

- Sharp for specific heat [12],
- Primenko and Van-Zee for conductivity [13 to 14],
- Scholze for the viscosity law [8],
- Cesar De Sa for the coefficients of convection with the ambient air [15].

The initial mould temperature is 150 °C.

6.2 Inverse method and identification procedure for the tests

The identification method used is based on an iterative diagram in three stages. The aim is to determine N parameters p_i in order to reduce the difference between the objective solution $\hat{f}$ and the numerical solution $f^*(p_1, p_2, ..., p_n)$. The error function E, to be minimized, is expressed by:

$$E(p_1, p_2, ..., p_n) = \frac{1}{2} \sum_{s=1}^{M} (r_s(p_1, p_2, ..., p_n))^2 \tag{8}$$

with

$$r_s(p_1, p_2, ..., p_n) = f_s^*(p_1, p_2, ..., p_n) - \hat{f}_s \tag{9}$$

and $i = 1, ..., N$

where M is the number of comparison points.

The resolution uses an iterative algorithm developed by Levenberg-Marquardt [20]. At iteration k, the corrections $\mathrm{d}p_i$ on the parameters p_i are obtained by the resolution of the following system:

$$[(J^k)^t J^k + \lambda^k \cdot I]\, \mathrm{d}p_i^k = - (J^k)^t r^k \tag{10}$$

where λ is the Levenberg-Marquardt parameter and I is the identity matrix with terms only on the diagonal equal to 1. The jacobian matrix J of the error function $E(p_1, p_2, ..., p_n)$ is expressed by:

$$J_{si} = \frac{\partial r_s}{\partial p_i} = \frac{\partial f_s^*}{\partial p_i} \tag{11}$$

with $s = 1, ..., M$ and $i = 1, ..., N$.

L_{si}, the terms of the jacobian matrix, are approximated by finite differences. A sensitivity coefficient S_p is added to the algorithm for the calculation of the partial derivative of each parameter:

$$\frac{\partial f^*(p_1, p_2, ..., p_n)}{\partial p_i} = \frac{f^*(p_i + \Delta p_i) - f^*(p_1, p_2, ..., p_n)}{\Delta p_i} \qquad (12)$$

with $\Delta p_i = p_i S_p$.

The Levenberg-Marquardt parameter λ simultaneously determines the direction and the size of the correction dp. Marquardt has shown that if this parameter tends to the infinite, the direction will take the greatest slope and the correction will be smaller.

The complete algorithm for the minimization of the error function $E(p_1, p_2, ..., p_n)$ (equation (8)) is:

- determination of the initial values of the parameters $p_i^{(0)}$, the sensitivity S_p and the Levenberg-Marquardt parameter $\lambda^{(0)}$;
- calculation of the numerical solution of the problem $f^*(p_1, p_2, ..., p_n)^{(0)}$, and determination of the error function $E(p_1, p_2, ..., p_n)^{(0)}$;
- for an iteration $k \geq 1$:

a) calculation of the jacobian matrix $J^{(k)}$ by solving an approximation by finite differences;

b) determination of the parameter corrections $dp_i^{(k)}$ by the resolution of the relation (10) and computation of $p_i^{(k+1)} = p_i^{(k)} + dp_i^{(k)}$;

c) calculation of the numerical solution of the problem $f^*(p_1, p_2, ..., p_n)^{(k+1)}$ and the error function $E(p_1, p_2, ..., p_n)^{(k+1)}$;

d) verification of the convergence of the solution $E(p_1, p_2, ..., p_n)^{(k+1)} < E(p_1, p_2, ..., p_n)^{(k)}$:

- if the convergence is checked and the error is lower than the stop criteria, the identification is finished,
- if the convergence is checked and the error is higher than the stop criteria, the identification continues (stage f),
- if the convergence is not checked, multiply the Levenberg-Marquardt parameter $\lambda^{(k)}$ by 10 and begin again at stage c);

f) reduction of the Levenberg-Marquardt parameter $\lambda^{(k)}$;
increment k to 1,
begin again at stage a).

E602P005

Contact:

Prof. D. Lochegnies
LAMIH
Université de Valenciennes
Le Mont Houy
F-59313 Valenciennes Cédex 9
E-mail: dominique.lochegnies@univ-valenciennes.fr